Dr. G. Smeets
Deutsch-Französisches Forschungsinstitut Saint-Louis

Institut Franco-Allemand de Recherches de Saint-Louis
5 Rue Du General Cassagnou
68301 Saint-Louis
FRANCE

Note
N 620/75

Density Profiles of a Subsonic Free Jet (D = 80 mm), Measured Using the Laser-Differential Interferometer

Saint-Louis
Nov. 5, 1975

Chief Engineer (Auriol)	Chairman at the BWB (Dr. Schall)

Translated from German by

Andreas R. Goetz
School of
Aeronautics & Astronautics
Purdue University
West Lafayette, IN 47906, USA

W. Lafayette, March 12, 1996

REPORT DOCUMENTATION PAGE

Form Approved
OMB No. 0704-0188

1. AGENCY USE ONLY (Leave blank)	2. REPORT DATE	3. REPORT TYPE AND DATES COVERED
	16 Apr 96	Translation

4. TITLE AND SUBTITLE
Density Profiles of a Subsonic Free Jet (D = 80 mm), Measured Using the Laser-Differential Interferometer

5. FUNDING NUMBERS
AFOSR Grant
F49620-94-1-0067

6. AUTHOR(S)
Author: G. Smeets, I.S.L., France.
Translated by Andreas Goetz, Purdue University

7. PERFORMING ORGANIZATION NAME(S) AND ADDRESS(ES)
Aerospace Sciences Lab.
3 Purdue University Airport
West Lafayette IN 47906-3371

8. PERFORMING ORGANIZATION REPORT NUMBER

9. SPONSORING/MONITORING AGENCY NAME(S) AND ADDRESS(ES)
Air Force Office of Scientific Research
110 Duncan Avenue
Bolling AFB
Washington DC 20332-0001

10. SPONSORING/MONITORING AGENCY REPORT NUMBER

11. SUPPLEMENTARY NOTES
Translation of Note N620/75, Institute Franco-Allemand de Recherches de Saint-Louis, Dr. G. Smeets, Nov. 1975. Translated by Mr. Andreas Goetz at Purdue University, School of Aeronautics and Astronautics, March 1996. Translation was corrected by G. Smeets.

12a. DISTRIBUTION/AVAILABILITY STATEMENT
Unclassified unlimited per original source document

12b. DISTRIBUTION CODE

13. ABSTRACT *(Maximum 200 words)*
A number of time-averaged density profiles of the cold subsonic free jet of the ISL were measured with the aid of a laser-differential interferometer. The primary goal of this investigation was to furnish proof by comparing the measured density profiles with readily available jet data, that is possible with little effort to determine the time-averaged refractive index profiles of a turbulent, axisymmetric free jet using the laser-differential interferometer. For the measurement, a laser-differential interferometer is described in detail.

14. SUBJECT TERMS
Laser interferometry, optical instrumentation

15. NUMBER OF PAGES
10 pages

16. PRICE CODE

17. SECURITY CLASSIFICATION OF REPORT	18. SECURITY CLASSIFICATION OF THIS PAGE	19. SECURITY CLASSIFICATION OF ABSTRACT	20. LIMITATION OF ABSTRACT
UNCLASSIFIED	UNCLASSIFIED	UNCLASSIFIED	UL

Contents page

Introduction

A number of time-averaged density profiles of the cold subsonic free jet of the ISL were measured with the aid of a laser-differential interferometer [1].

The primary goal of this investigation was to furnish proof by comparing the measured density profiles with readily available jet data, that it is possible with little effort to determine the time-averaged refractive index profiles of a turbulent, axisymmetric free jet using the laser-differential interferometer. The application of the measurement technique to hot jets and jets of larger diameter poses no problems.

By combining the measured density profiles with measured velocity profiles, the profiles of all flow properties - e.g. the Mach number distribution - can be determined experimentally, constant, known pressure provided.

Measurement Technique

For the measurement, a laser-differential interferometer as described in detail in [2] is employed. In this case, the optical arrangement (fig. 1) is quite simple. The beam separation is very small. It measures a = 0.16 mm and is oriented normal to the free jet axis. The lens #2 and the cylinder lenses #3 and #4 form the laserlight into bands at the free jet location, extending over more than 1 cm in the direction of the flow, but less than 0.5 mm in the normal direction. With this spatial averaging method it is possible to reduce the signal fluctuations due to turbulence.

Since the free jet can be traversed horizontally as well as vertically, translation of the laserlight path or the whole interferometer is superfluous. The optical path gradients $\partial\phi/\partial y(y)$ were registered by a xy-plotter. The vertical free jet position was linearly coupled to the y-position of the plotter. One run lasted about 15 seconds.

Between the resulting signal ΔU and the optical path gradient $\partial\phi/\partial y$, the following relationship exists:

$$\Delta U = \pi \cdot U_0 \frac{a}{\lambda} \frac{\partial\phi}{\partial y}, \tag{1}$$

where a denotes the beam separation distance, λ is the laserlight wavelength, and U_0 the interference amplitude. Due to the spatial light band averaging and an additional time-averaging with the bandwidth limited to ≤ 10 Hz, the fluctuating part of the optical path gradients is strongly reduced. Such geometrical and electrical averaging will be permissible only, if the signal content of every single light ray is confined within its full bandwidth to the applicable range of eqn. (1), that is, if no overshooting the linear range of the interference slope takes place. To ensure this, the signal fluctuations were measured with a thin pair of laser beams within the full bandwidth. It turned out that the crucial condition

$$\frac{|\Delta U|}{U_0} \le \frac{1}{4} \tag{2}$$

was practically always fulfilled.

In order to calculate the refractive index distribution *n(r)*, Abel's formula was used:

$$n(r) - n_0 = -\frac{1}{\pi} \int_r^{\infty} \frac{\frac{\partial \phi}{\partial y}(y)}{\sqrt{y^2 - r^2}} dy . \tag{3}$$

The gradient profiles were smoothened and the two asymmetrical branches were merged to one single curve of $\partial\phi / \partial y$ over y > 0. After inserting into eqn (3), this curve was used for the numerical computation of *n(r)* and $\Delta\rho(r)$ for the respective jet cross section.

Results

The resulting profiles $\Delta\rho(r)$ are depicted in fig. 3. They all possess the plateau expected for the jet core. This is a first hint for the reliability of the measurement technique. For more in-depth examination, the densities measured in the jet core were compared with estimations from jet data. The following relation exists between the density increase in the inner of the jet $\Delta\rho/\rho_N$ and the stagnation properties T_0 and p_0:

$$\frac{\Delta\rho}{\rho_N} = \frac{p}{p_N} \cdot \left[\frac{T_N}{T_0} \left(\frac{p_0}{p} \right)^{\frac{2}{7}} - \frac{T_N}{T_1} \right] \tag{4}$$

p_N and T_N are standard pressure and temperature, T_1 the ambient temperature and p the pressure assumed to be equal in the jet and in the environment. While the stagnation pressure p_0 was measured fairly precisely, the stagnation temperature was uncertain by some °C and moreover changed during the jet run-time. In the table below, the measured density increases in the core of the jet are compared to the values $\Delta\rho/\rho_N$ computed using (4).

x [cm]	p_0 [mbar]	T_0 [°C]	$\Delta\rho/\rho_N$(th.)	$\Delta\rho/\rho_N$(exp.)	
2	1783	18 - 14	0.195 - 0.180	0.178	Eqn. (4) is valid for T_0, T_1, T_N in [K]
10	1783	18 - 14	0.195 - 0.180	0.166	
18	1783	16 - 11.5	0.187 - 0.205	0.187	
26	1783	17 - 12	0.184 - 0.203	0.198	
10	1813	18 - 10	0.185 - 0.216	0.212	
10	1513	17 - 10	0.134 - 0.159	0.167	
10	1278	11.5 - 8.5	0.104 - 0.115	0.115	

The pressure p was 993 mbar, the ambient temperature T_1 = 22 °C ± 1 °C.

The measured and the estimated density increases in the jet core largely agree. A preciser comparison is precluded by the uncertainty and the change over time of the measured stagnation temperature.

It was attempted to compute the velocity profiles at the edge of the free jet from the density profiles in fig. 3 using Crocco's relation:

$$\frac{u}{u_1} = \frac{H - h_1}{H_0 - h_1} . \tag{5}$$

Crocco's equation implies the assumption that in the turbulent mixing region at the edge of the jet the order of magnitude of momentum exchange and energy transport is the same, that is, the turbulent Prandtl number is unity. Under this assumption Crocco's relation is valid for turbulent free jets of the same gas as their outer environment. u_1 and H_0 denote the velocity and stagnation enthalpy in the jet core, $H = h + 1/2 \cdot u^2$ the local (time-averaged) stagnation enthalpy at the edge of the jet, and h_1 the ambient static enthalpy.

The values of u_1 and H_0 were calculated from p_0 and the measured Values of $\Delta\rho/\rho_N$ in the jet core - that is without using the measured values of T_0 by applying the ideal gas law. Fig. 4 shows the resulting velocity profiles.

Conclusive Remarks

The results agree with the jet core density predictions. They show the expected plateau and lie within the estimated density range with respect to the uncertainty limits for T_0.

Further tests will compare the velocity profiles computed from the density profiles to directly measured velocities using laser anemometry techniques.

Literature

[1] G. Koerber
Laser Anemometry. A Contribution to the Reliability Tests of a New Technique for Velocity Measurements in a Gas Flow.
(Contribution à l'étude de la fiabilité d'une nouvelle méthode de mesure de vitesses dans un écoulement gazeux: la vélocimétrie laser.)
(Die Laseranemometrie. Ein Beitrag zu der Prüfung der Zuverlässigkeit einer neuen Methode für Geschwindigkeitsmessungen in einer Gasströmung.)
ISL - R 132/75.

[2] G. Smeets, A. George
Applications of the Laser-Differential Interferometer in Gas Dynamics.
(Anwendungen des Laser-Differentialinterferometers in der Gasdynamik.)
(Application de l'interféromètre différentiel en lumière laser à laa dynamique des gaz.)
ISL - 28/73.

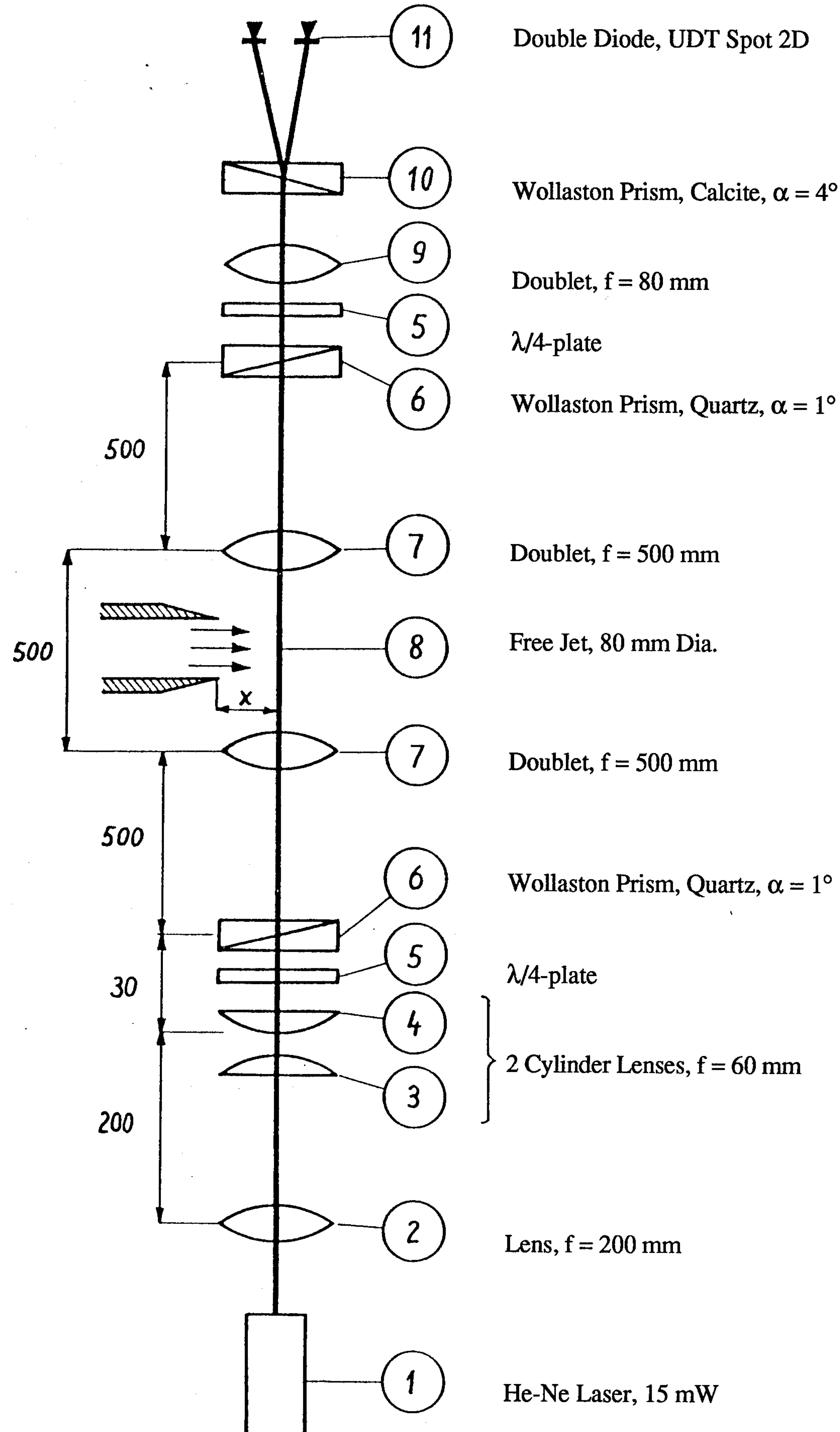
11
Double Diode, UDT Spot 2D
10
Wollaston Prism, Calcite, α = 4°
9
Doublet, f = 80 mm
5
λ/4-plate
6
Wollaston Prism, Quartz, α = 1°
500
7
Doublet, f = 500 mm
500
8
Free Jet, 80 mm Dia.
x
7
Doublet, f = 500 mm
500
6
Wollaston Prism, Quartz, α = 1°
5
λ/4-plate
30
4
2 Cylinder Lenses, f = 60 mm
3
200
2
Lens, f = 200 mm
1
He-Ne Laser, 15 mW

Fig. 1

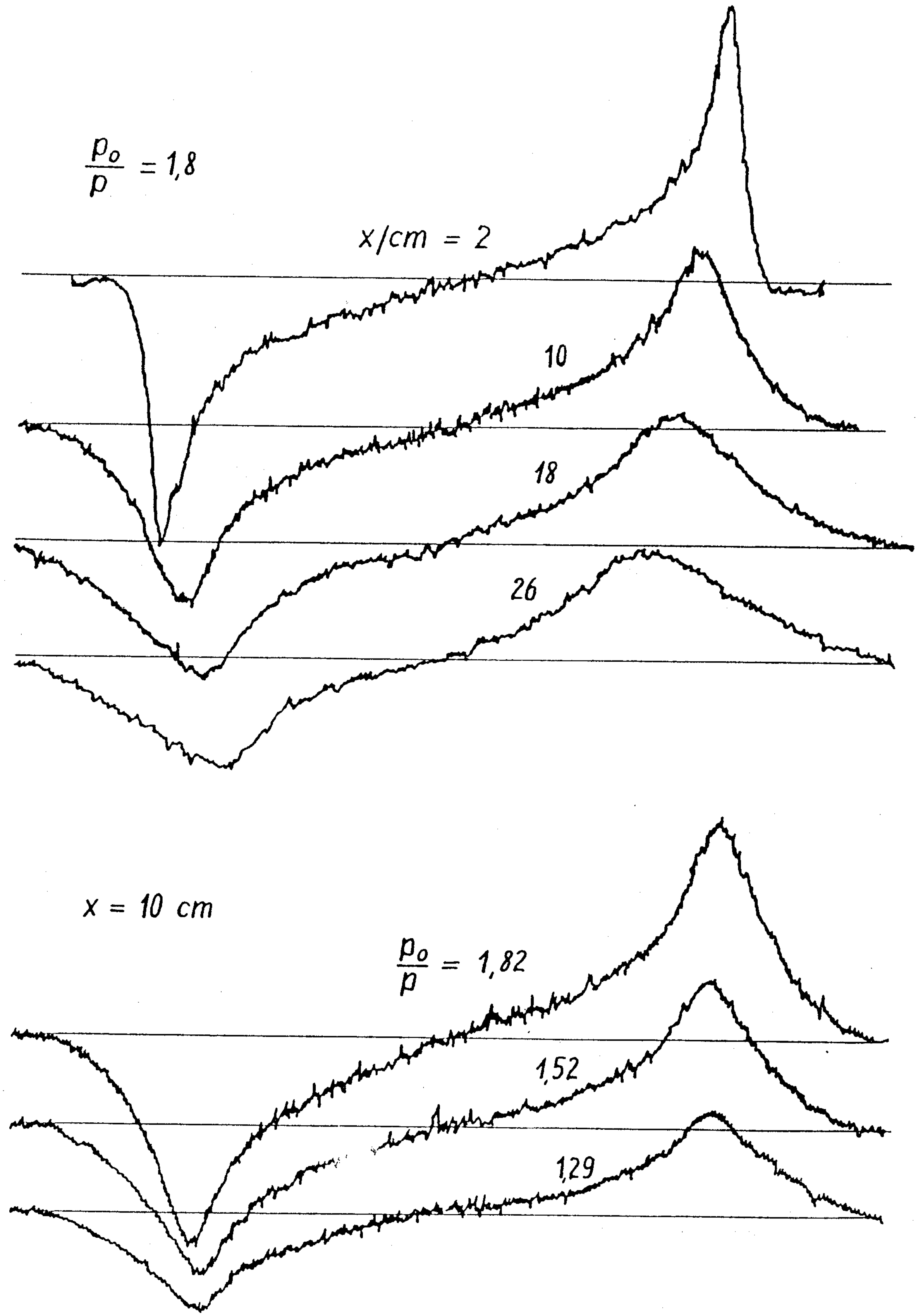

Fig. 2

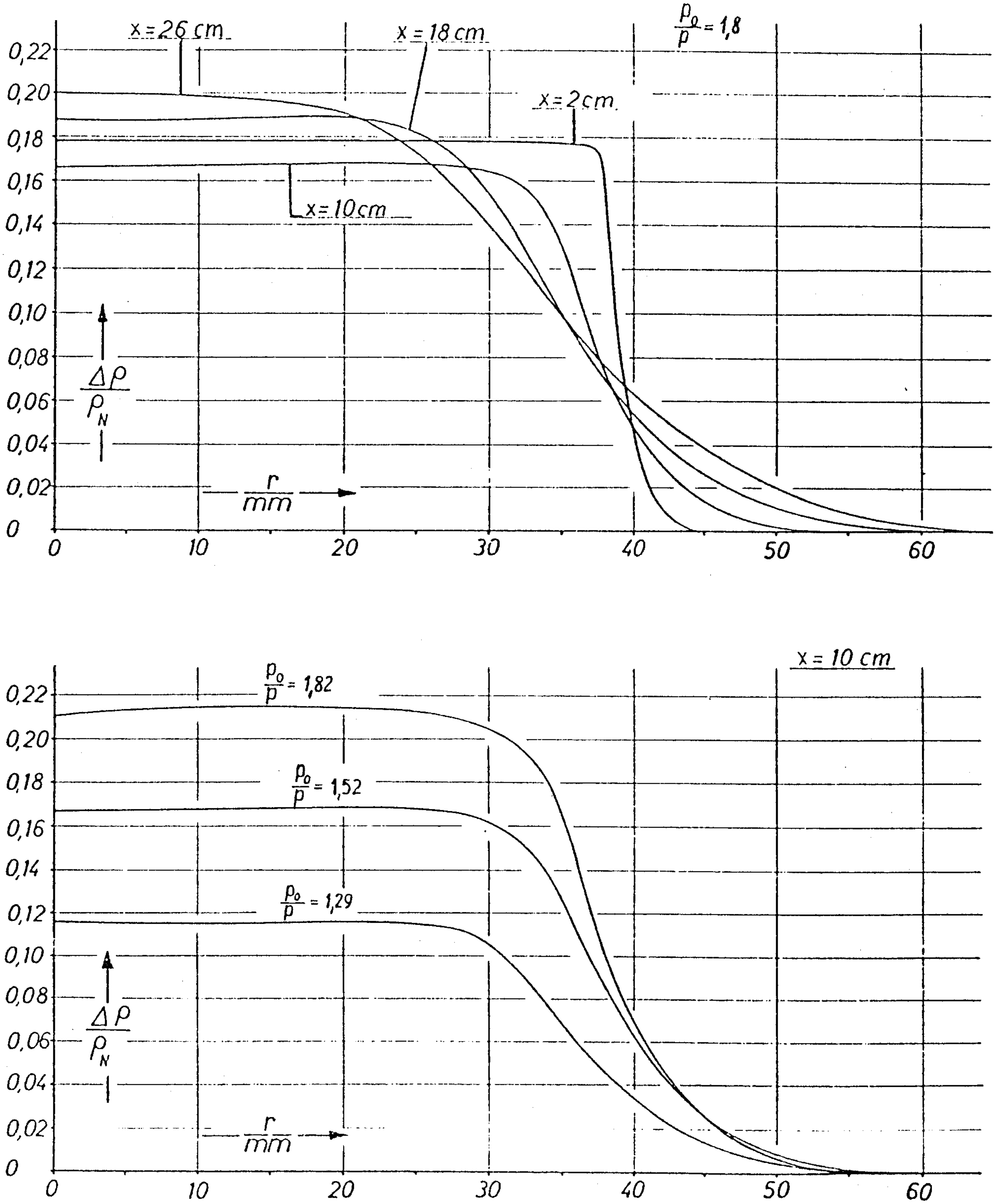
x = 26 cm
x = 18 cm
$\frac{p_0}{p} = 1{,}8$
x = 2 cm
x = 10 cm
$\frac{\Delta \rho}{\rho_N}$
$\frac{r}{mm}$
0,22
0,20
0,18
0,16
0,14
0,12
0,10
0,08
0,06
0,04
0,02
0
0
10
20
30
40
50
60
x = 10 cm
$\frac{p_0}{p} = 1{,}82$
$\frac{p_0}{p} = 1{,}52$
$\frac{p_0}{p} = 1{,}29$

Fig. 3

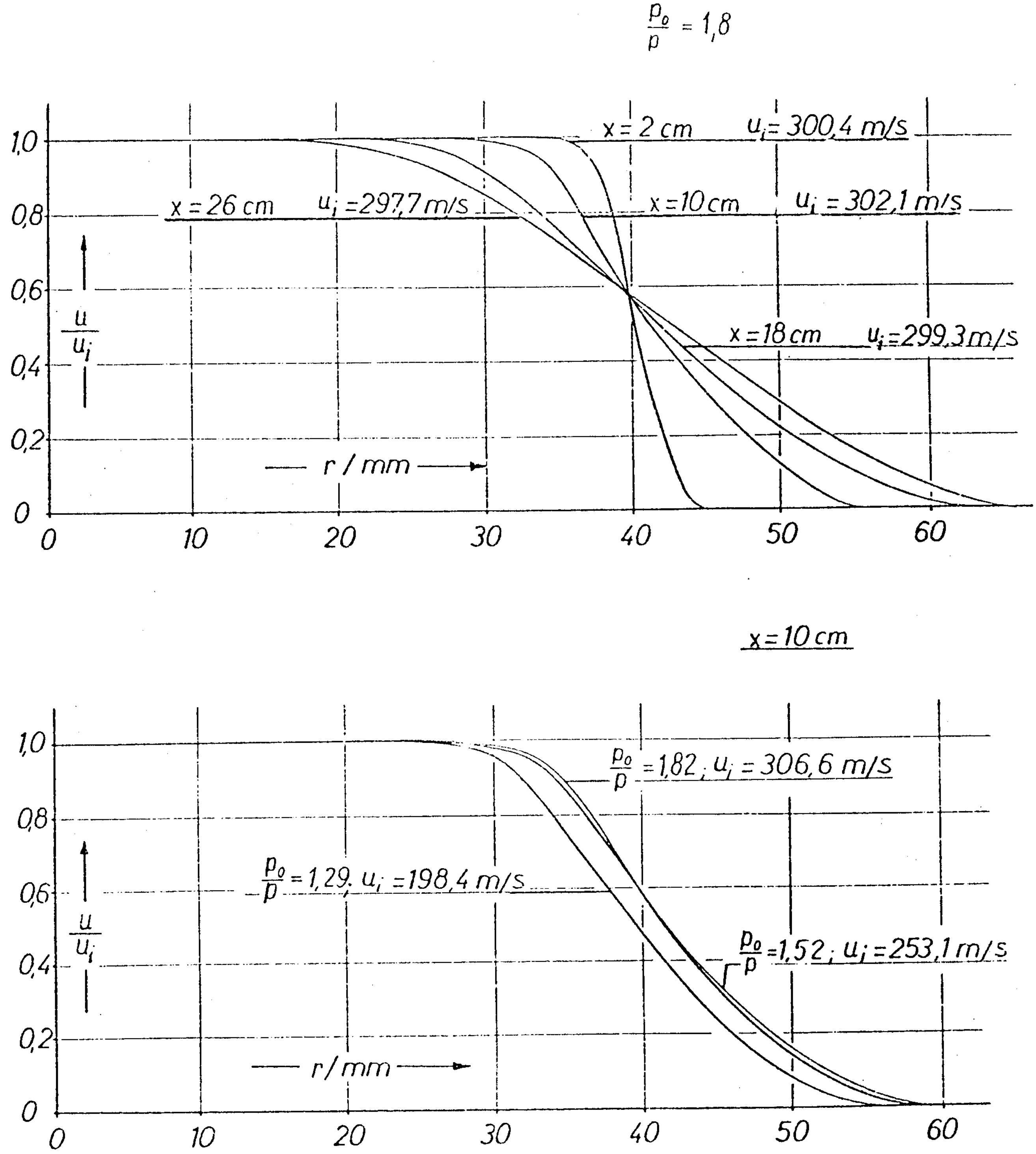

$\frac{p_0}{p} = 1{,}8$
x = 2 cm u_i = 300,4 m/s
x = 26 cm u_i = 297,7 m/s
x = 10 cm u_i = 302,1 m/s
x = 18 cm u_i = 299,3 m/s
$\frac{u}{u_i}$
r / mm
x = 10 cm
$\frac{p_0}{p}$ = 1,82 ; u_i = 306,6 m/s
$\frac{p_0}{p}$ = 1,29 ; u_i = 198,4 m/s
$\frac{p_0}{p}$ = 1,52 ; u_i = 253,1 m/s
$\frac{u}{u_i}$
r / mm

Fig. 4